Bioorganic Chemistry 159 (2025) 108354

Contents lists available at ScienceDirect

Bioorganic Chemistry

journal homepage: www.elsevier.com/locate/bioorg

Hydroxytyrosol *N*-alkylcarbamate conjugates as antitrypanosomal and antileishmanial agents

Belinda Jimenez-Martin [a,1], Diego A. Guerra-Arias [b,c,1], Antonio Martinez [a], Raquel García-Hernández [b], Marta Medina-O'Donnell [a], José María Pérez-Victoria [b,*], Francisco Rivas [a,*]

[a] Departamento de Quimica Organica. Facultad de Ciencias, Universidad de Granada, E-18071 Granada, Spain
[b] Instituto de Parasitología y Biomedicina "Lopez-Neyra", CSIC, (IPBLN-CSIC), PTS Granada, Avda. del Conocimiento, 17, 18016, Armilla, Spain
[c] Programa de Estudio y Control de Enfermedades Tropicales PECET, Faculty of Medicine, University of Antioquia, Medellín 050010, Colombia

ARTICLE INFO

Keywords:
Hydroxytyrosol
Carbamate group
Antitrypanosomal
Antileishmanial

ABSTRACT

Novel lipophilic hydroxytyrosol *N*-alkylcarbamate conjugates were synthesized by coupling several alkyl isocyanates of different chain lengths with the primary hydroxy group of this natural phenol. These *N*-alkylcarbamate conjugates were tested as antitrypanosomal and antileishmanial agents, and their cytotoxicity was evaluated against the human MRC-5 and THP-1 cell lines. Five of these *N*-alkylcarbamate derivatives showed submicromolar IC_{50} concentrations against *Trypanosoma brucei brucei*, with values ranging from 0.2 to 0.8 μM, and three other hydroxytyrosol conjugates showed IC_{50} values below 5 μM. Data for the five most active *N*-alkylcarbamate derivatives indicate a gain in activity relative to hydroxytyrosol of between 115- and 460-fold, and selectivity indices for control/human MRC-5 cells relative to *T. b. brucei* parasites of between 47- and 140-fold. These *N*-alkylcarbamate derivatives were also tested against the intracellular amastigote form of *Leishmania donovani* in infected THP-1 macrophages, where five compounds had IC_{50} values less than or equal to 10 μM, with selectivity indices relative to L. *donovani* of between 3- and 25-fold in MRC-5 cells and between 8- and 60-fold in THP-1 cells. In all of these derivatives, the ortho-diphenolic groups were free. When the hydroxytyrosol derivatives had *ortho*-diphenolic groups protected by benzyl groups, cytotoxicity against *T. b. brucei* and L. *donovani* showed significantly higher IC_{50} values, with most cases exceeding 20 μM.

1. Introduction

Protozoan parasites cause infectious diseases that threaten millions of lives in subtropical and tropical areas around the globe [1,2]. Human African Trypanosomiasis (HAT), triggered by *Trypanosoma brucei* and transmitted by the tsetse fly, is responsible for sleeping sickness, which threatens 70 million people in sub-Saharan Africa and affects productive livestock and domestic animal-based farming [3,4]. *Trypanosoma brucei brucei* is a hemoflagellate subspecies of this parasitic protozoa that causes nagana, a disease of African cattle, which is commonly used in studies with these parasites, as they apparently do not infect humans and are easy to culture. Leishmaniasis, caused by different species of *Leishmania* and transmitted by sand flies, poses a major health problem worldwide. Visceral leishmaniasis is the most severe type of disease and is caused by species such as *Leishmania donovani* and *Leishmania infantum* [5,6]. Treatments for these neglected diseases have major limitations, such as high toxicity and increased resistance [7]. Consequently, there is a vital need to develop new antiparasitic therapies.

Natural phenols are compounds containing at least one phenol group. These compounds form a large group of secondary metabolites of mostly plant or microbial origin, which exhibit a wide variety of biological properties, including antioxidant, anti-inflammatory, antitumor, antiviral, and antineurodegenerative activities [8–12].

Hydroxytyrosol (HT) is a phenolic alcohol that can be isolated from a high percentage of industrial olive-oil waste. This phenolic compound exhibits several promising pharmacological activities with great potential as an anticancer, anti-inflammatory, neuroprotective, cardioprotective, antioxidant, and antimicrobial agent [13–16].

* Corresponding authors at: Departamento de Química Orgánica. Facultad de Ciencias, Universidad de Granada, E-18071 Granada, Spain (F. Rivas); Instituto de Parasitología y Biomedicina "Lopez-Neyra", CSIC, (IPBLN-CSIC), PTS Granada, Avda. del Conocimiento, 17, 18016, Armilla, Spain.
E-mail addresses: josepv@ipb.csic.es (J.M. Pérez-Victoria), frivas@ugr.es (F. Rivas).
[1] B. J.-M. and D.A. G.-A. are co-first authors

https://doi.org/10.1016/j.bioorg.2025.108354
Received 31 January 2025; Received in revised form 2 March 2025; Accepted 5 March 2025
Available online 12 March 2025

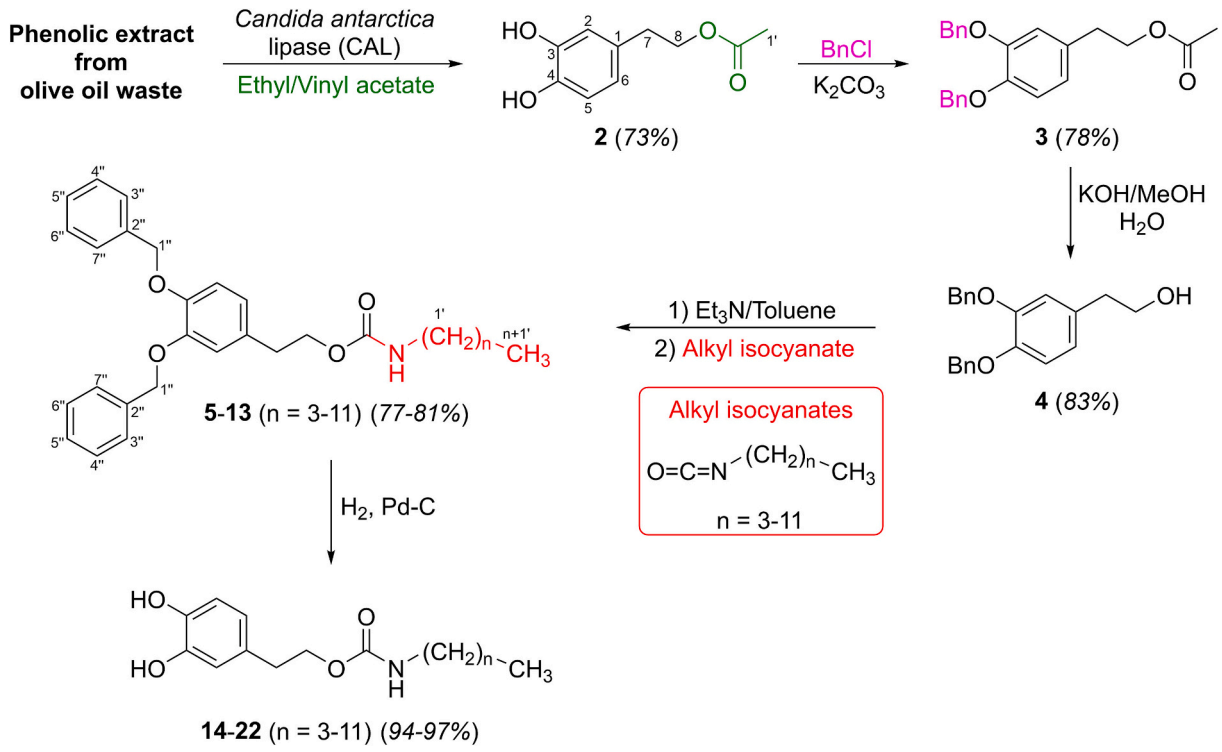

Scheme 1. Synthesis of hydroxytyrosol *N*-alkylcarbamate conjugates.

In recent years, natural phenols have attracted great interest in various sectors, such as the pharmaceutical industry, owing to their beneficial effects on health. However, these compounds, such as HT, have certain drawbacks, such as their solubility and bioavailability, due to their hydrophilicity, so they have rarely been used as active ingredients in pharmaceuticals. Consequently, a number of more lipophilic derivatives have recently been developed on the primary hydroxy group of HT, such as esters [17–21], carbonates [22,23], and ethers [24–26] with different alkyl chains. Some of these more lipophilic derivatives of hydroxytyrosol are more active than HT and have remarkable antioxidant, anti-inflammatory, antiproliferative, or neuroprotective properties [17,20,27]. Recently, some more lipophilic HT derivatives have also been reported to have antitrypanosomal [28] and antileishmanial properties [29].

Compounds with a carbamate group have been widely used in new drug discovery [30]. The carbamate group is a hybrid between an amide and an ester with good chemical stability, ease of crossing cell membranes, and potential for improved biological and pharmacokinetic properties. Recently, some hydroxytyrosol carbamate derivatives have been reported as antiradical and antimicrobial agents [31].

In this study, a series of hydroxytyrosol *N*-alkylcarbamate conjugates with different chain lengths were prepared. In addition, these derivatives were tested as antitrypanosomal and antileishmanial agents, and their cytotoxicity against a healthy cell line (MRC-5) and a macrophage cell line (THP-1) was determined.

2. Results and discussion

2.1. Chemistry

Hydroxytyrosol (**1**, HT), a phenolic alcohol belonging to the group of natural phenols, is used as a raw material for the synthesis of conjugates. This phenolic compound is distributed in many plants, but especially in wastes from the olive-oil industry, where it has been isolated.

Several hydroxytyrosol *N*-alkylcarbamate conjugates were synthesized for testing as antitrypanosomal and antileishmanial agents (Scheme 1). Enzymatic treatment of the phenolic extract of olive-oil wastes with *Candida antarctica* lipase (CAL) and ethyl/vinyl acetate was used to isolate hydroxytyrosol from this phenolic mixture while protecting its primary hydroxy group. In this reaction, hydroxytyrosol acetate (**2**) was isolated [23]. Compound **2** was first treated with benzyl chloride (BnCl) and K_2CO_3 in acetone to protect its *ortho*-diphenolic groups, yielding derivative **3**, and subsequently with KOH/MeOH/H_2O to deprotect its primary hydroxy group, giving dibenzylated hydroxytyrosol (**4**, DBHT). Compound **4** was then treated with triethylamine (Et_3N) in toluene under an Ar atmosphere to facilitate the coupling reactions with various alkyl isocyanates of different chain lengths (from butyl isocyanate to dodecyl isocyanate). In these coupling reactions, a set of dibenzylated hydroxytyrosol *N*-alkylcarbamate conjugates (**5**–**13**) was prepared (77–81 %).

The ^{1}H NMR spectra of compounds **5**–**13** showed the characteristic signals of dibenzylated hydroxytyrosol (**4**, DBHT), such as those corresponding to two monosubstituted phenyl groups (between δ_H 7.3 and 7.5), to two benzylated oxygenated methylene groups (around δ_H 5.15), to three aromatic proton signals (H-2, H-5, and H-6, between δ_H 6.7 and 6.9), to one benzylated methylene group (H-7, around δ_H 2.8), and to one benzylated oxygenated methylen group (H-8, around δ_H 4.2). In addition, these ^{1}H NMR spectra showed the signals of the corresponding alkyl chain attached to the carbamate group. These signals were a triplet due to the methyl group of the alkyl chain (around δ_H 0.9), several multiplets (between δ_H 1.2 and 1.5) attributable to the methylene groups in the center of the chain, a quadruplet (around δ_H 3.15) corresponding to the methylene group (2H-1′) adjacent to the nitrogen atom of the carbamate group, and the hydrogen of the carbamate function (between δ_H 4.5 and 4.6). The ^{13}C NMR spectra of these compounds (**5**–**13**) showed, among the signals of compound **4** (DBHT) [23], that of a nitrogenated methylene carbon (C-1′, around δ_C 41), several signals from the methylene groups in the center of the alkyl chain (between δ_C 20 and 32), a signal from the methyl group of the alkyl chain (around δ_C 14), and the signal from the carbamate carbon (δ_C 156.6).

Catalytic hydrogenation of these dibenzylated hydroxytyrosol *N*-alkylcarbamate conjugates (**5**–**13**) produced the corresponding

Table 1
Trypanocidal activity and cytotoxicity of dibenzylated hydroxytyrosol *N*-alkylcarbamate conjugates **5**–**13**.

Compound #	n[a]	*T. b. brucei* IC_{50} (μM)	MRC-5 IC_{50} (μM)	SI[b]	AG[c]	ClogP[d]
DBHT (4)	–	27.2 ± 1.4	58.8 ± 8.1	2	1	4.53
5	3	17.3 ± 0.8	> 200	> 12	2	6.72
6	4	14.4 ± 1.0	> 200	> 14	2	7.25
7	5	> 20	> 200	–	–	7.78
8	6	> 20	> 200	–	–	8.31
9	7	> 20	> 200	–	–	8.84
10	8	> 20	> 200	–	–	9.37
11	9	> 20	> 200	–	–	9.89
12	10	> 20	> 200	–	–	10.42
13	11	> 20	> 200	–	–	10.95
Suramin	–	0.024 ± 0.001	> 200	> 8333	–	–
	–	–		–	–	–

[a] n = Number of methylene groups (CH_2) of the alkyl chain.
[b] SI = Selectivity Index (IC_{50} MRC-5 / IC_{50} *T. b. brucei*).
[c] AG = Activity gain (IC_{50} DBHT (**4**) *T. b. brucei* / IC_{50} compound # *T. b. brucei*).
[d] ClogP = Calculated logP values using the ChemDraw Professional 21.0 software.

derivatives (**14**–**22**). The benzyl protecting groups of the dibenzylated derivatives **5**–**13** were removed with H_2 and Pd − C in EtOH, with yields above 95 % (Scheme 1). Comparing the spectroscopic data of derivatives **14**–**22** and their corresponding dibenzylated derivatives **5**–**13**, the only difference in the spectra of the former was precisely the absence of signals from these benzyl groups. In these derivatives (**14**–**22**), the ^1H NMR spectra showed the signals of three aromatic protons (H-2, H-5, and H-6, between δ_H 6.6 and 6.8), of a benzylated methylene group (H-7, around δ_H 2.8), of a benzylated oxygenated methylene group (H-8, around δ_H 4.2), of the methyl group of the alkyl chain (around δ_H 0.9), of the methylene groups of the alkyl chain center (between δ_H 1.3 and 1.5), of the methylene group adjacent to the nitrogen atom of the carbamate group (2H-1′, around δ_H 3.15), and of the hydrogen atom of the carbamate function (between δ_H 4.8 and 4.9). The ^{13}C NMR spectra of these derivatives (**14**–**22**) showed, in addition to the signals of compound **1** (HT), that of a nitrogenated methylene carbon (C-1′, around δ_C 41), several signals from the methylene groups in the center of the alkyl chain (between δ_C 20 and 32), a signal from the methyl group of the alkyl chain (around δ_C 14), and the signal from the carbon atom of the carbamate group (δ_C 157). The assignment of these signals was performed with the help of HSQC and HMBC spectra.

2.2. Biological activity

The antitrypanosomal and antileishmanial activity of dibenzylated hydroxytyrosol (**5**–**13**) or hydroxytyrosol (**14**–**22**) *N*-alkylcarbamate conjugates was evaluated *in vitro* against the bloodstream forms of *T. b. brucei*, as well as against the intracellular amastigote forms of L. *donovani* (MHOM/67/HU3), to calculate the respective IC_{50} concentrations (50 % inhibition of parasite growth). This last study was performed with the intramacrophageal amastigote forms of L. *donovani* because this stage is the clinically relevant one, since it is the one residing in the infected person and, therefore, more appropriate in the search for leishmaniacidal compounds. The cytotoxicity of these conjugates was also evaluated against MRC-5, a human lung fibroblast cell line widely used as a control for drug toxicity [29,32,33], as well as against THP-1, a monocytic leukemia cell line. Suramin and miltefosine were used as positive drug controls. Suramin is used against the first stage of African trypanosomiasis caused by *Trypanosoma brucei rhodesiense*, although it may have adverse effects [34]. Miltefosine is used for the treatment of visceral, cutaneous and mucocutaneous leishmaniasis and is currently the only oral drug licensed for the treatment of this disease [35].

Table 2
Antileishmanial activity and cytotoxicity of dibenzylated hydroxytyrosol *N*-alkylcarbamate conjugates **5**–**13**.

Compound #	Amastigotes *L. donovani* IC_{50} (μM)	MRC-5 IC_{50} (μM)	THP-1 IC_{50} (μM)	SI[a] (MRC-5)	SI[b] (THP-1)	AG[c]
DBHT (**4**)	> 20	58.8 ± 8.1	77.0 ± 0.4	< 3	< 4	1
5	> 20	> 200	91.7 ± 5.8	–	< 5	–
6	> 20	> 200	> 200	–	–	–
7	> 20	> 200	> 200	–	–	–
8	> 20	> 200	> 200	–	–	–
9	> 20	> 200	> 200	–	–	–
10	> 20	> 200	189 ± 1.0	–	< 9	–
11	> 20	> 200	> 200	–	–	–
12	> 20	> 200	110 ± 6.0	–	< 6	–
13	> 20	> 200	> 200	–	–	–
Miltefosine	0.48 ± 0.07	66.99 ± 2.34	17.97 ± 1.80	140	99	–

[a] SI (MRC-5) = Selectivity Index (IC_{50} MRC-5 / IC_{50} *L. donovani*).
[b] SI (THP-1) = Selectivity Index (IC_{50} THP-1 / IC_{50} *L. donovani*).
[c] AG = Activity gain (IC_{50} DBHT (**4**) *L. donovani* / IC_{50} compound # *L. donovani*).

Table 3
Trypanocidal activity and cytotoxicity of hydroxytyrosol *N*-alkylcarbamate conjugates **14**–**22**.

Compound #	n[a]	*T. b. brucei* IC_{50} (μM)	MRC-5 IC_{50} (μM)	SI[b]	AG[c]	ClogP[d]
HT (**1**)	–	92.1 ± 1.2	> 200	> 2	1	0.07
14	3	22.2 ± 1.0	142.3 ± 1.9	6	4	2.26
15	4	3.3 ± 0.8	95.7 ± 4.3	29	28	2.79
16	5	2.6 ± 0.7	84.9 ± 3.4	33	35	3.32
17	6	2.0 ± 0.1	63.6 ± 3.3	32	46	3.85
18	7	0.8 ± 0.1	37.4 ± 0.5	47	115	4.38
19	8	0.4 ± 0.1	35.6 ± 1.0	89	230	4.91
20	9	0.3 ± 0.1	42.0 ± 2.4	140	307	5.44
21	10	0.2 ± 0.0	22.0 ± 0.2	110	460	5.97
22	11	0.3 ± 0.0	18.2 ± 0.3	61	307	6.49

[a] n = Number of methylene groups (CH_2) of the alkyl chain.
[b] SI = Selectivity Index (IC_{50} MRC-5 / IC_{50} *T. b. brucei*).
[c] AG = Activity gain (IC_{50} HT (**1**) *T. b. brucei* / IC_{50} compound # *T. b. brucei*).
[d] ClogP = Calculated logP values using the ChemDraw Professional 21.0 software.

Treatment with miltefosine killed the intracellular amastigote form of L. *donovani* [36].

The IC_{50} concentration values of derivatives **5**–**13** against *T. b. brucei* parasites were, in most cases, higher than 20 μM, except for the derivatives with the shortest *N*-alkyl chain (**5**, 17.3 μM; and **6**, 14.4 μM). Their cytotoxicity was also tested against the healthy cell line MRC-5, reaching IC_{50} values above 200 μM for all derivatives (Table 1). These results indicate that, in general, these derivatives (**5**–**13**), whose *ortho*-phenolic groups were protected with a benzyl group, were neither antitrypanosomal against *T. b. brucei* nor cytotoxic against the healthy cell line MRC-5.

The IC_{50} values of derivatives **5**–**13** against the amastigote form of L. *donovani* were higher than 20 μM, while those against the healthy cell line MRC-5 were greater than 200 μM. Only a few derivatives (**5**, 91.7 μM; **10**, 189 μM; and **12**, 110 μM) had IC_{50} values lower than 200 μM, but above 90 μM, against THP-1 macrophage cells (Table 2). Therefore, these dibenzylated hydroxytyrosol *N*-alkylcarbamate conjugates (**5**–**13**) were neither antileishmanial nor cytotoxic against healthy MRC-5 or THP-1 macrophages.

Table 3 shows the trypanocidal and cytotoxic data for the reference compound (HT, **1**) and its *N*-alkylcarbamate derivatives (**14**–**22**). IC_{50}

Table 4
Antileishmanial activity and cytotoxicity of hydroxytyrosol *N*-alkylcarbamate conjugates **14**–**22**.

Compound #	Amastigotes L. *donovani* IC_{50} (μM)	THP-1 IC_{50} (μM)	SI[a] (MRC-5)	SI[b] (THP-1)	AG[c]
HT (**1**)	> 20	> 200	–	–	–
14	> 20	> 200	< 7	–	–
15	> 20	> 200	< 5	–	–
16	3.4 ± 1.1	> 200	25	> 59	> 6
17	11.0 ± 2.9	165.0 ± 0.8	6	15	> 2
18	10.2 ± 1.5	81.2 ± 0.9	4	8	> 2
19	9.4 ± 0.7	76.3 ± 1.2	4	8	> 2
20	17.6 ± 3.3	73.8 ± 0.4	2	4	> 1
21	7.0 ± 0.3	68.0 ± 1.6	3	10	> 3
22	14.2 ± 2.6	27.5 ± 4.2	1	2	> 1

[a] SI (MRC-5) = Selectivity Index (IC_{50} MRC-5 (Table 3) / IC_{50} *L. donovani*).
[b] SI (THP-1) = Selectivity Index (IC_{50} THP-1 / IC_{50} *L. donovani*).
[c] AG = Activity gain (IC_{50} HT (**1**) *L. donovani* / IC_{50} compound # *L. donovani*).

concentration values against *T. b. brucei* were generally below 5 μM, except for the derivative with the shortest *N*-alkyl chain (**14**), which was slightly above 20 μM. Five of these derivatives with the longest *N*-alkyl chain (**18**–**22**) showed submicromolar IC_{50} values (0.2–0.8 μM), with activity gains (AG) relative to HT (**1**) ranging from 115- to 460-fold. The other three derivatives (**15**–**17**) showed slightly higher values (2.0–3.3 μM), with 28- to 46-fold increases in the activity (AG). The cytotoxicity of these derivatives (**14**–**22**) was also tested against the healthy MRC-5 cell line, with the most active derivatives (**18**–**22**) showing selectivity indices (SI) of MRC-5 cells relative to *T. b. brucei* parasites of between 47- and 140-fold. The activity of Suramin (IC_{50} = 0.024 μM), the positive control used against *T. b. brucei*, is 10-fold higher than that of some of the HT derivatives tested (**20**–**22**). However, this compound frequently produces nephrotoxicity and peripheral neuropathy. In addition, it does not cross the blood-brain barrier so it is only administered for the first stage of sleeping sickness [34].

Table 4 presents the antileishmanial and cytotoxic data for the reference compound (HT, **1**) and the same *N*-alkylcarbamate derivatives (**14**–**22**). Five of these HT conjugates (**16**–**19** and **21**), with free *ortho*-diphenolic groups and medium-sized *N*-alkyl chains, showed IC_{50} values less than or equal to 10 μM, registering selectivity indices (SI), relative to L. *donovani* parasites, of 3- to 25-fold with healthy MRC-5 cells, and of 8- to 60-fold with THP-1 macrophages. The activity of Miltefosine (IC_{50} = 0.48 μM), the positive control used against the amastigote form of L. *donovani*, is 7-fold higher than that of derivative **16** (IC_{50} = 3.4 μM), but Mitelfosine is more cytotoxic against MRC-5 and THP-1 cell lines. In addition, Miltefosine is teratogenic and embryotoxic, even at low concentrations [35].

The calculated partition coefficient (ClogP) values for the hydroxytyrosol *N*-alkylcarbamate conjugates (**14**–**22**) were estimated using ChemDraw Professional 21.0 software in an attempt to understand the higher activity of these derivatives with respect to the reference compound (HT, **1**). The more lipophilic character of these HT derivatives (ClogP = 2.26–6.49) with respect to HT itself (ClogP = 0.77) may be related to the greater ability of these HT derivatives to cross parasite cell membranes [37]. On the other hand, the dibenzylated hydroxytyrosol *N*-alkylcarbamate conjugates (**5**–**13**) have a much more pronounced lipophilic character, with very high ClogP values (ClogP = 6.72–10.95), which may explain their low activity.

The use of hit and lead criteria in drug discovery for infectious diseases from the GHIT Fund has helped to identify potential candidates for future research [38]. Some of the synthesized derivatives meet quite a few of these criteria, such as structures confirmed by spectroscopic and spectrometric identification, purity above 95 %, synthesized in 5 steps from the natural compound with quite acceptable yields, submicromolar IC_{50} values or at least below 10 μM and selectivity indices between 25- and 140-fold. These promising candidates would be derivatives **20** (IC_{50} = 0.3 μM, SI = 140, AG = 307) and **21** (IC_{50} = 0.2 μM, SI = 110, AG = 460) against *T. b. brucei* parasites and derivative **16** (IC_{50} = 3.4 μM, SI_{MRC-5} = 25, SI_{THP-1} > 59, AG > 6) against L. *donovani* parasites.

3. Conclusions

Nine dibenzylated hydroxytyrosol (**5**–**13**) and nine hydroxytyrosol (**14**–**22**) *N*-alkylcarbamate conjugates were synthesized by a coupling reaction with nine alkyl isocyanates, of different chain lengths, with the primary hydroxy group of HT.

An analysis was made of the antitrypanosomal (*T. b. brucei*) and antileishmanial (*L. donovani*) properties, as well as their cytotoxicity against a healthy cell line (MRC-5) and a macrophage cell line (THP-1), of these dibenzylated hydroxytyrosol (**5**–**13**) or hydroxytyrosol (**14**–**22**) *N*-alkylcarbamate conjugates. Five of these *N*-alkylcarbamate derivatives (**18**–**22**), with longer *N*-alkyl chains, had submicromolar IC_{50} concentrations against *T. b. brucei*, with values ranging from 0.2 to 0.8 μM, and three other hydroxytyrosol conjugates (**15**–**17**), with shorter *N*-alkyl chains, showed IC_{50} values below 5 μM. These five most active *N*-alkylcarbamate derivatives (**18**–**22**) exhibited activity gains (AG) relative to hydroxytyrosol of 115- to 460-fold and had selectivity indices (SI) of healthy MRC-5 cells relative to *T. b. brucei* parasites of 47- to 140-fold. The *ortho*-diphenolic groups of these derivatives were free; therefore, this characteristic and the presence of an *N*-alkyl chain are decisive in the activity of these compounds.

These *N*-alkylcarbamate derivatives (**5**–**22**) were also tested against the amastigote form of L. *donovani*, where five compounds (**16**–**19** and **21**), with medium-sized *N*-alkyl chains and free *ortho*-diphenolic groups, had IC_{50} values less than or equal to 10 μM, with selectivity indices (SI), relative to L. *donovani* parasites, of 3- to 25-fold increase in healthy MRC-5 cells, and of 8- to 60-fold increase in THP-1 macrophages. In the hydroxytyrosol conjugates **5**–**13**, with the *ortho*-diphenolic groups were protected by benzyl groups, cytotoxicity against *T. b. brucei* and L. *donovani* showed significantly higher IC_{50} values, in most cases above 20 μM.

The results of these HT *N*-alkylcarbamate derivatives against *T. b. brucei* in comparison with those of other previously published derivatives, such as HT alkyl esters [29] and HT alkylcarbonates [28], led to the conclusion that the activity gain data (AG) relative to hydroxytyrosol and the selectivity index data (SI) are slightly better, indicating that the *N*-alkylcarbamate derivatives are more active and less cytotoxic. The structure of all these HT derivatives implies that the conjugates with higher antitrypanosomal activity should have free *ortho*-diphenolic groups of HT, and the alkyl chain should have a medium-high length (6–12 carbon atoms). In consideration of the antileishmanial results, they are also better than those reported for HT alkyl esters [29].

Hydroxytyrosol *N*-alkylcarbamate conjugates **20** and **21** against *T. b. brucei* parasites and derivative **16** against L. *donovani* parasites are potential candidates for further studies to investigate their possible mechanisms of action.

4. Experimental

4.1. General experimental chemical procedures

The FTIR spectra were recorded using a Mattson Satellite FTIR spectrometer, and the NMR spectra using a Bruker Avance Neo spectrometer (^{1}H, 400 MHz; ^{13}C, 100 MHz) with $CDCl_3$ as the solvent. The ^{13}C NMR chemical shifts were determined using DEPT with a flip angle of 135°. The purity of the new compounds was measured using a Waters Acquity UPLC system coupled with a Waters Synapt G2 HRMS spectrometer with ESI. The purity of all compounds was confirmed to be ≥95 %. Merck silica-gel 60 aluminum sheets (1.16835) were used for TLC, while Merck silica gel 60 (0.040–0.063 mm, 1.09385) was used for flash chromatography. CH_2Cl_2 (Fisher, D/1852/17) with increasing

Table 5
^{1}H NMR (400 MHz) and ^{13}C NMR (100 MHz) spectroscopic data of compounds **5**–**7**.

No.	5		6		7	
	δ_C, mult.	δ_H (*J* in Hz)	δ_C, mult.	δ_H (*J* in Hz)	δ_C, mult.	δ_H (*J* in Hz)
1	131.7, C		131.7, C		131.7, C	
2	116.2, CH	6.84, d (2.0)	116.2, CH	6.83, d (2.2)	116.2, CH	6.83, d (2.1)
3	147.8, C		149.1, C		149.1, C	
4	149.1, C		147.8, C		147.8, C	
5	115.5, CH	6.89, d (8.2)	115.5, CH	6.88, br d (8.1)	115.5, CH	6.88, d (8.2)
6	121.9, CH	6.75, dd (8.2, 2.0)	121.9, CH	6.74, dd (8.1, 2.2)	121.9, CH	6.74, dd (8.2, 2.1)
7	35.2, CH_2	2.83, t (7.0)	35.2, CH_2	2.82, t (7.1)	35.2, CH_2	2.82, t (7.0)
8	65.3, CH_2	4.22, t (7.0)	65.3, CH_2	4.21, t (7.1)	65.3, CH_2	4.21, t (7.0)
OCONH	156.6, C		156.6, C		156.6, C	
NH		4.61, br s		4.59, br s		4.58, br s
1″	71.6, CH_2	5.14, s	71.6, CH_2	5.14, s	71.6, CH_2	5.14, s
1″	71.5, CH_2	5.16, s	71.5, CH_2	5.15, s	71.5, CH_2	5.15, s
2″	137.6, C		137.6, C		137.6, C	
2″	137.5, C		137.5, C		137.5, C	
3″ & 7″	127.5, CH	7.47–7.42, m	127.5, CH	7.48–7.43, m	127.5, CH	7.48–7.43, m
3″ & 7″	127.4, CH	7.47–7.42, m	127.4, CH	7.48–7.43, m	127.4, CH	7.48–7.43, m
4″ & 6″	128.6, CH	7.38–7.33, m	128.6, CH	7.38–7.34, m	128.6, CH	7.38–7.34, m
5″	127.8, CH	7.32, m	127.9, CH	7.34, m	127.9, CH	7.34, m
1′	40.8, CH_2	3.16, q (7.3)	41.1, CH_2	3.15, q (7.0)	41.1, CH_2	3.15, q (6.8)
2′	32.2, CH_2	1.47, quint (7.3)	29.8, CH_2	1.48, quint (7.0)	30.1, CH_2	1.48, m
3′	20.0, CH_2	1.34, sex (7.3)	29.0, CH_2	1.29, m	26.5, CH_2	1.30, m
4′	13.8, CH_3	0.93, t (7.3)	22.5, CH_2	1.33, m	31.6, CH_2	1.30, m
5′			14.1, CH_3	0.91, t (7.0)	22.7, CH_2	1.30, m
6′					14.1, CH_3	0.89, t (6.7)

Recorded at ^{1}H NMR 400 MHz and ^{13}C NMR 100 MHz in $CDCl_3$.

amounts of acetone (Fisher, A/0600/17) was used as the eluent. All the solvents had an analytical reagent-grade purity. Novo-Nordisk Bio-industrial S.A. (Madrid, Spain) kindly supplied *Candida antarctica* lipase (CAL).

4.2. Enzymatic acetylation of hydroxytyrosol (1)

From the solid by-products of olive milling, a polar extract composed mainly of phenolic compounds was isolated by a patented procedure and called the phenolic extract [39]. To this phenolic extract (3 g), a mixture of 30 mL of ethyl acetate and 60 mL of vinyl acetate with *Candida antarctica* lipase (3 g) was added. This mixture was stirred for 24 h at 40 °C with orbital shaking. The reaction mixture was filtered and evaporated under reduced pressure, yielding a residue that was purified by column chromatography, isolating hydroxytyrosol acetate (**2**, 2.78 g, 14.2 mmol, 73 %) [23].

4.3. Benzylation of hydroxytyrosol acetate (2)

This benzylation reaction was carried out with 2.5 g (12.7 mmol) of hydroxytyrosol acetate (**2**) dissolved in dry acetone (20 mL), followed by the addition of K_2CO_3 (6 g, 43.4 mmol) and BnCl (3 mL). The reaction mixture was stirred under reflux for 4 h, then filtered, and the solvent was evaporated under reduced pressure. The residue was dissolved in CH_2Cl_2 and washed three times with water. The organic layer was dried with anhydrous Na_2SO_4, filtered, and concentrated until dry. The residue was purified by column chromatography, yielding dibenzylated derivative **3** (3.76 g, 10.0 mmol, 78 %).

4.3.1. 3,4-Bis(benzyloxy)phenethyl acetate (3)

Colorless oil; IR (ν_{max}) 3031, 2967, 1736, 1605, 1519, 1248, 1100, 738, 697 cm^{-1}; ^{1}H NMR data: δ_H 7.47–7.45 (4H, m, H-3″ and H-7″), 7.38–7.37 (4H, m, H-4″ and H-6″), 7.32 (2H, m, H-5″), 6.89 (1H, d, *J* = 8.0 Hz, H-5), 6.84 (1H, d, *J* = 2.1 Hz, H-2), 6.75 (1H, dd, *J* = 8.0, 2.1 Hz, H-6), 5.16 and 5.15 (4H, s, H-1″), 4.22 (2H, t, *J* = 7.2 Hz, H-8), 2.84 (2H, t, *J* = 7.2 Hz, H-7), 2.02 (3H, s, H-1′). ^{13}C NMR data: δ_C 171.1 (C, OCONH), 149.0 (C, C-3), 147.8 (C, C-4), 137.5 and 137.4 (C, 2C-2″), 131.3 (C, C-1), 128.6 (CH, 4C-4″), 127.9 (CH, 2C-5″), 127.4 (CH, 4C-3″), 121.9 (CH, C-6), 116.1 (CH, C-2), 115.3 (CH, C-5), 71.5 (CH_2, 2C-1″), 65.1 (CH_2, C-8), 34.7 (CH_2, C-7), 21.1 (CH_3, C-1′); HRESIMS *m/z* 399.1568 $[M + Na]^+$ (calcd for $C_{24}H_{24}O_4Na^+$, 399.1572).

4.4. Deacetylation of derivative 3

Derivative **3** (3 g, 7.5 mmol) was dissolved in 80 mL of a mixture of CH_3OH/H_2O (70 %) and KOH (5 %) and then refluxed for 1 h. Subsequently, the reaction mixture was extracted with CH_2Cl_2, dried in anhydrous Na_2SO_4, and evaporated to dryness. Chromatography on a silica gel column yielded derivative **4** (2.22 g, 6.6 mmol, 83 %) [23].

4.5. Synthesis of dibenzylated hydroxytyrosol N-alkylcarbamate conjugates (5–13)

Dibenzylated hydroxytyrosol (**4**, DBHT, 0.5 mmol) and triethylamine (Et_3N, 0.4 mmol) were dissolved in 50 mL of toluene to form a reaction mixture under an Ar atmosphere. On the other hand, different alkyl isocyanates (0.6 mmol) were prepared in toluene (5 mL) under an Ar atmosphere. Then, each alkyl isocyanate solution was added slowly to the corresponding reaction mixture. Each reaction mixture was heated at reflux for 10 h. Afterwards, the solvent was evaporated, and the residue was purified by chromatography to give conjugates **5**–**13** (77–81 %).

According to the general procedure, compound **4** (0.5 mmol) was coupled with butyl isocyanate (0.6 mmol), pentyl isocyanate (1.0 mmol), hexyl isocyanate (1.0 mmol), heptyl isocyanate (1.0 mmol), octyl isocyanate (1.0 mmol), nonyl isocyanate (1.0 mmol), decyl isocyanate (1.0 mmol), undecyl isocyanate (1.0 mmol), or dodecyl isocyanate (1.0 mmol) to give the respective conjugates (**5**–**13**). These compounds were purified by column chromatography to yield 172 mg (0.4 mmol, 79 %) of **5**, 178 mg (0.4 mmol, 80 %) of **6**, 183 mg (0.4 mmol, 79 %) of **7**, 190 mg (0.4 mmol, 80 %) of **8**, 198 mg (0.4 mmol, 81 %) of **9**, 202 mg (0.4 mmol, 80 %) of **10**, 205 mg (0.4 mmol, 79 %) of **11**, 208 mg (0.4 mmol, 78 %) of **12**, and 211 mg (0.4 mmol, 77 %) of **13**.

4.5.1. 3,4-Bis(benzyloxy)phenethyl butylcarbamate (5)

Colorless crystal, m.p. 71–73 °C; IR (ν_{max}) 3316, 3062, 3032, 2927, 1686, 1544, 1520, 1260, 1232, 1137, 1020, 729, 693 cm^{-1}; ^{1}H and ^{13}C NMR data see Table 5; HRESIMS *m/z* 456.2147 $[M + Na]^+$ (calcd for

Table 6
^{1}H NMR (400 MHz) and ^{13}C NMR (100 MHz) spectroscopic data of compounds **8**–**10.**

No.	8		9		10	
	δ_C, mult.	δ_H (*J* in Hz)	δ_C, mult.	δ_H (*J* in Hz)	δ_C, mult.	δ_H (*J* in Hz)
1	131.7, C		131.6, C		131.7, C	
2	116.2, CH	6.83, d (2.1)	116.2, CH	6.83, d (2.0)	116.2, CH	6.83, d (2.0)
3	149.1, C		149.0, C		149.1, C	
4	147.8, C		147.8, C		147.8, C	
5	115.5, CH	6.88, d (8.1)	115.4, CH	6.88, d (8.2)	115.5, CH	6.88, d (8.2)
6	121.9, CH	6.74, dd (8.1, 2.1)	121.9, CH	6.74, dd (8.2, 2.0)	121.9, CH	6.74, dd (8.2, 2.0)
7	35.2, CH_2	2.82, t (7.1)	35.2, CH_2	2.82, t (7.0)	35.2, CH_2	2.82, t (7.0)
8	65.3, CH_2	4.21, t (7.1)	65.3, CH_2	4.20, t (7.0)	65.3, CH_2	4.21, t (7.0)
OCONH	156.6, C		156.6, C		156.6, C	
NH		4.57, br s		4.57, br s		4.57, br s
1″	71.6, CH_2	5.14, s	71.6, CH_2	5.14, s	71.6, CH_2	5.14, s
1″	71.5, CH_2	5.15, s	71.5, CH_2	5.15, s	71.5, CH_2	5.15, s
2″	137.6, C		137.6, C		137.6, C	
2″	137.5, C		137.5, C		137.5, C	
3″ & 7″	127.5, CH	7.48–7.42, m	127.5, CH	7.47–7.43, m	127.5, CH	7.48–7.42, m
3″ & 7″	127.4, CH	7.48–7.42, m	127.4, CH	7.47–7.43, m	127.4, CH	7.48–7.42, m
4″ & 6″	128.6, CH	7.39–7.33, m	128.6, CH	7.39–7.33, m	128.6, CH	7.39–7.33, m
5″	127.9, CH	7.31, m	127.9, CH	7.33–7.28, m	127.9, CH	7.33–7.27, m
1′	41.1, CH_2	3.15, q (6.8)	41.1, CH_2	3.15, q (6.8)	41.1, CH_2	3.14, q (6.8)
2′	30.1, CH_2	1.48, m	30.1, CH_2	1.48, m	30.2, CH_2	1.47, m
3′	26.8, CH_2	1.30, m	26.9, CH_2	1.30, m	26.9, CH_2	1.29, m
4′	29.1, CH_2	1.30, m	29.3, CH_2	1.28, m	29.4, CH_2	1.27, m
5′	31.9, CH_2	1.29, m	29.4, CH_2	1.28, m	29.4, CH_2	1.27, m
6′	22.7, CH_2	1.29, m	31.9, CH_2	1.26, m	29.6, CH_2	1.27, m
7′	14.2, CH_3	0.89, t (6.9)	22.8, CH_2	1.29, m	32.0, CH_2	1.26, m
8′			14.2, CH_3	0.89, t (6.9)	22.8, CH_2	1.29, m
9′					14.2, CH_3	0.89, t (6.8)

Recorded at ^{1}H NMR 400 MHz and ^{13}C NMR 100 MHz in $CDCl_3$.

Table 7
^{1}H NMR (400 MHz) and ^{13}C NMR (100 MHz) spectroscopic data of compounds **11**–**13.**

No.	11		12		13	
	δ_C, mult.	δ_H (*J* in Hz)	δ_C, mult.	δ_H (*J* in Hz)	δ_C, mult.	δ_H (*J* in Hz)
1	131.7, C		131.7, C		131.6, C	
2	116.2, CH	6.83, d (2.1)	116.2, CH	6.83, d (2.1)	116.2, CH	6.84, d (2.1)
3	149.1, C		149.1, C		149.0, C	
4	147.8, C		147.8, C		147.8, C	
5	115.5, CH	6.88, d (8.1)	115.4, CH	6.88, d (8.2)	115.4, CH	6.88, d (8.2)
6	121.9, CH	6.74, dd (8.1, 2.1)	121.9, CH	6.74, dd (8.2, 2.1)	121.9, CH	6.74, dd (8.2, 2.1)
7	35.2, CH_2	2.82, t (7.1)	35.2, CH_2	2.82, t (7.1)	35.2, CH_2	2.82, t (7.1)
8	65.3, CH_2	4.20, t (7.1)	65.3, CH_2	4.21, t (7.0)	65.3, CH_2	4.21, t (7.1)
OCONH	156.6, C		156.6, C		156.6, C	
NH		4.57, br s		4.58, br s		4.60, br s
1″	71.6, CH_2	5.13, s	71.6, CH_2	5.14, s	71.6, CH_2	5.14, s
1″	71.5, CH_2	5.15, s	71.5, CH_2	5.15, s	71.5, CH_2	5.15, s
2″	137.6, C		137.6, C		137.6, C	
2″	137.5, C		137.5, C		137.5, C	
3″ & 7″	127.5, CH	7.48–7.42, m	127.5, CH	7.48–7.42, m	127.5, CH	7.48–7.42, m
3″ & 7″	127.4, CH	7.48–7.42, m	127.4, CH	7.48–7.42, m	127.4, CH	7.48–7.42, m
4″ & 6″	128.6, CH	7.39–7.33, m	128.6, CH	7.39–7.33, m	128.6, CH	7.39–7.33, m
5″	127.9, CH	7.33–7.27, m	127.9, CH	7.33–7.27, m	127.9, CH	7.33–7.27, m
1′	41.2, CH_2	3.14, q (6.8)	41.1, CH_2	3.15, q (6.8)	41.1, CH_2	3.15, q (6.7)
2′	30.2, CH_2	1.47, m	30.1, CH_2	1.48, m	30.1, CH_2	1.48, m
3′	26.9, CH_2	1.29, m	26.9, CH_2	1.30, m	26.9, CH_2	1.30, m
4′	29.4, CH_2	1.27, m	29.4, CH_2	1.27, m	29.4, CH_2	1.27, m
5′	29.4, CH_2	1.27, m	29.5, CH_2	1.27, m	29.5, CH_2	1.27, m
6′	29.7, CH_2	1.27, m	29.7, CH_2	1.27, m	29.8, CH_2	1.27, m
7′	29.7, CH_2	1.27, m	29.7, CH_2	1.27, m	29.7, CH_2	1.27, m
8′	32.0, CH_2	1.27, m	29.7, CH_2	1.27, m	29.7, CH_2	1.27, m
9′	22.8, CH_2	1.29, m	32.0, CH_2	1.26, m	29.7, CH_2	1.27, m
10′	14.2, CH_3	0.89, t (6.8)	22.8, CH_2	1.32, m	32.0, CH_2	1.27, m
11′			14.2, CH_3	0.89, t (6.8)	22.8, CH_2	1.32, m
12′					14.2, CH_3	0.90, t (6.8)

Recorded at ^{1}H NMR 400 MHz and ^{13}C NMR 100 MHz in $CDCl_3$.

$C_{27}H_{31}NO_4Na^+$, 456.2151).

4.5.2. 3,4-Bis(benzyloxy)phenethyl pentylcarbamate (6)

Colorless crystal, m.p. 72–74 °C; IR (ν_{max}) 3315, 3063, 3032, 2927, 1687, 1545, 1520, 1262, 1233, 1137, 1022, 729, 693 cm^{-1}; ^{1}H and ^{13}C NMR data see Table 5; HRESIMS *m/z* 470.2307 $[M + Na]^+$ (calcd for $C_{28}H_{33}NO_4Na^+$, 470.2307).

Table 8
^{1}H NMR (400 MHz) and ^{13}C NMR (100 MHz) spectroscopic data of compounds **14–16.**

No.	14		15		16	
	δ_C, mult.	δ_H (*J* in Hz)	δ_C, mult.	δ_H (*J* in Hz)	δ_C, mult.	δ_H (*J* in Hz)
1	130.3, C		130.2, C		130.4, C	
2	115.9, CH	6.73, d (2.1)	115.9, CH	6.73, d (2.1)	115.9, CH	6.73, d (2.1)
3	144.0, C		144.1, C		144.0, C	
4	142.8, C		142.9, C		142.8, C	
5	115.4, CH	6.78, d (8.0)	115.4, CH	6.78, d (8.1)	115.4, CH	6.78, d (8.0)
6	121.2, CH	6.59, dd (8.0, 2.1)	121.1, CH	6.57, dd (8.1, 2.1)	121.2, CH	6.59, dd (8.0, 2.1)
7	35.0, CH_2	2.78, t (7.1)	34.9, CH_2	2.76, t (7.1)	35.0, CH_2	2.78, t (7.1)
8	65.9, CH_2	4.21, t (7.1)	66.0, CH_2	4.20, t (7.1)	65.9, CH_2	4.21, t (7.1)
OCONH	157.3, C		157.4, C		157.3, C	
NH		4.81, br s		4.91, br s		4.80, br s
1′	40.9, CH_2	3.15, q (7.3)	41.2, CH_2	3.13, q (6.8)	41.2, CH_2	3.15, q (6.7)
2′	32.0, CH_2	1.45, quint (7.3)	29.6, CH_2	1.46, quint (6.8)	30.0, CH_2	1.47, m
3′	20.0, CH_2	1.31, sext (7.3)	28.9, CH_2	1.24, m	26.5, CH_2	1.29, m
4′	13.8, CH_3	0.90, t (7.3)	22.4, CH_2	1.28, m	31.6, CH_2	1.29, m
5′			14.1, CH_3	0.87, t (7.0)	22.7, CH_2	1.29, m
6′					14.1, CH_3	0.88, t (6.8)

Recorded at ^{1}H NMR 400 MHz and ^{13}C NMR 100 MHz in $CDCl_3$.

4.5.3. 3,4-Bis(benzyloxy)phenethyl hexylcarbamate (7)

Colorless crystal, m.p. 73–75 °C; IR (ν_{max}) 3333, 3064, 3036, 2928, 1682, 1538, 1515, 1253, 1224, 1134, 1006, 740, 696 cm^{-1}; ^{1}H and ^{13}C NMR data see Table 5; HRESIMS *m/z* 484.2458 $[M + Na]^+$ (calcd for $C_{29}H_{35}NO_4Na^+$, 484.2464).

4.5.4. 3,4-Bis(benzyloxy)phenethyl heptylcarbamate (8)

Colorless crystal, m.p. 74–76 °C; IR (ν_{max}) 3312, 3063, 3033, 2922, 1686, 1545, 1519, 1260, 1232, 1137, 1022, 728, 693 cm^{-1}; ^{1}H and ^{13}C NMR data see Table 6; HRESIMS *m/z* 498.2615 $[M + Na]^+$ (calcd for $C_{30}H_{37}NO_4Na^+$, 498.2620).

4.5.5. 3,4-Bis(benzyloxy)phenethyl octylcarbamate (9)

Colorless crystal, m.p. 84–86 °C; IR (ν_{max}) 3330, 3065, 3038, 2923, 1685, 1538, 1513, 1249, 1231, 1132, 1006, 723, 696 cm^{-1}; ^{1}H and ^{13}C NMR data see Table 6; HRESIMS *m/z* 512.2782 $[M + Na]^+$ (calcd for $C_{31}H_{39}NO_4Na^+$, 512.2777).

4.5.6. 3,4-Bis(benzyloxy)phenethyl nonylcarbamate (10)

Colorless crystal, m.p. 85–87 °C; IR (ν_{max}) 3323, 3064, 3036, 2920, 1685, 1542, 1513, 1254, 1231, 1134, 1007, 738, 696 cm^{-1}; ^{1}H and ^{13}C NMR data see Table 6; HRESIMS *m/z* 526.2946 $[M + Na]^+$ (calcd for $C_{32}H_{41}NO_4Na^+$, 526.2933).

4.5.7. 3,4-Bis(benzyloxy)phenethyl decylcarbamate (11)

Colorless crystal, m.p. 86–88 °C; IR (ν_{max}) 3319, 3062, 3036, 2918, 1685, 1540, 1516, 1258, 1232, 1136, 1010, 729, 695 cm^{-1}; ^{1}H and ^{13}C NMR data see Table 7; HRESIMS *m/z* 540.3097 $[M + Na]^+$ (calcd for $C_{33}H_{43}NO_4Na^+$, 540.3090).

Table 9
^{1}H NMR (400 MHz) and ^{13}C NMR (100 MHz) spectroscopic data of compounds **17–19.**

No.	17		18		19	
	δ_C, mult.	δ_H (*J* in Hz)	δ_C, mult.	δ_H (*J* in Hz)	δ_C, mult.	δ_H (*J* in Hz)
1	130.2, C		130.2, C		130.2, C	
2	115.9, CH	6.73, d (2.1)	115.9, CH	6.73, d (2.0)	115.9, CH	6.73, d (2.1)
3	144.1, C		144.1, C		144.1, C	
4	142.9, C		142.9, C		142.9, C	
5	115.4, CH	6.78, d (8.0)	115.4, CH	6.78, d (8.1)	115.4, CH	6.78, d (8.1)
6	121.1, CH	6.58, dd (8.0, 2.1)	121.2, CH	6.58, dd (8.1, 2.0)	121.1, CH	6.58, dd (8.1, 2.1)
7	34.9, CH_2	2.77, t (7.2)	34.9, CH_2	2.77, t (7.1)	34.9, CH_2	2.76, t (7.2)
8	66.0, CH_2	4.21, t (7.2)	66.0, CH_2	4.21, t (7.1)	66.0, CH_2	4.20, t (7.2)
OCONH	157.4, C		157.4, C		157.4, C	
NH		4.86, br s		4.84, br s		4.88, br s
1′	41.2, CH_2	3.14, q (6.8)	41.3, CH_2	3.15, q (6.7)	41.2, CH_2	3.14, q (6.7)
2′	30.0, CH_2	1.46, m	30.0, CH_2	1.46, m	29.9, CH_2	1.45, m
3′	26.8, CH_2	1.27, m	26.9, CH_2	1.27, m	26.8, CH_2	1.27, m
4′	29.0, CH_2	1.27, m	29.3, CH_2	1.26, m	29.4, CH_2	1.26, m
5′	31.8, CH_2	1.26, m	29.3, CH_2	1.26, m	29.4, CH_2	1.26, m
6′	22.7, CH_2	1.26, m	31.9, CH_2	1.25, m	29.6, CH_2	1.26, m
7′	14.2, CH_3	0.87, t (6.8)	22.8, CH_2	1.28, m	32.0, CH_2	1.26, m
8′			14.2, CH_3	0.88, t (6.8)	22.8, CH_2	1.29, m
9′					14.2, CH_3	0.88, t (6.8)

Recorded at ^{1}H NMR 400 MHz and ^{13}C NMR 100 MHz in $CDCl_3$.

4.5.8. 3,4-Bis(benzyloxy)phenethyl undecylcarbamate (12)

Colorless crystal, m.p. 86–89 °C; IR (ν_{max}) 3318, 3060, 3034, 2917, 1684, 1550, 1520, 1266, 1233, 1137, 1022, 729, 693 cm^{-1}; ^{1}H and ^{13}C NMR data see Table 7; HRESIMS *m/z* 554.3266 $[M + Na]^+$ (calcd for $C_{34}H_{45}NO_4Na^+$, 554.3246).

4.5.9. 3,4-Bis(benzyloxy)phenethyl dodecylcarbamate (13)

Colorless crystal, m.p. 87–89 °C; IR (ν_{max}) 3317, 3059, 3030, 2916, 1688, 1548, 1520, 1268, 1233, 1137, 1023, 730, 694 cm^{-1}; ^{1}H and ^{13}C NMR data see Table 7; HRESIMS *m/z* 568.3418 $[M + Na]^+$ (calcd for $C_{35}H_{47}NO_4Na^+$, 568.3403).

4.6. Synthesis of hydroxytyrosol N-alkylcarbamate conjugates (14–22)

Compounds **5**–**13** (0.25 mmol) were separately dissolved in EtOH (10 mL), and 20 mg of Pd—C were added. The reaction mixture was hydrogenated at 5 atm of H_2 pressure for 24 h. Each solution was filtered, and each organic layer was concentrated under reduced pressure. Each residue was purified by column chromatography to yield derivatives **14**–**22** (94–97 %).

According to the general procedure described above, each dibenzylated hydroxytyrosol *N*-alkylcarbamate conjugate **5** (108 mg), **6** (112 mg), **7** (115 mg), **8** (119 mg), **9** (122 mg), **10** (126 mg), **11** (129 mg), **12** (133 mg), or **13** (136 mg) was debenzylated with H_2/Pd-C to give, respectively, **14** (60 mg, 0.24 mmol, 96 %), **15** (65 mg, 0.24 mmol, 97 %), **16** (68 mg, 0.24 mmol, 97 %), **17** (70 mg, 0.24 mmol, 95 %), **18** (74

Table 10
^{1}H NMR (400 MHz) and ^{13}C NMR (100 MHz) spectroscopic data of compounds **20**–**22**.

No.	20		21		22	
	δ_C, mult.	δ_H (*J* in Hz)	δ_C, mult.	δ_H (*J* in Hz)	δ_C, mult.	δ_H (*J* in Hz)
1	130.2, C		130.2, C		130.3, C	
2	115.9, CH	6.73, br s	115.9, CH	6.73, d (2.1)	115.9, CH	6.73, d (2.1)
3	144.1, C		144.1, C		144.0, C	
4	142.9, C		142.9, C		142.9, C	
5	115.4, CH	6.78, d (8.1)	115.4, CH	6.78, d (8.1)	115.4, CH	6.78, d (8.1)
6	121.1, CH	6.58, br d (8.1)	121.1, CH	6.58, dd (8.1, 2.1)	121.2, CH	6.59, dd (8.1, 2.1)
7	34.9, CH_2	2.77, t (7.2)	34.9, CH_2	2.78, t (7.2)	35.0, CH_2	2.78, t (7.2)
8	66.0, CH_2	4.20, t (7.2)	66.0, CH_2	4.21, t (7.2)	66.0, CH_2	4.21, t (7.2)
OCONH	157.4, C		157.4, C		157.3, C	
NH		4.87, br s		4.86, br s		4.82, br s
1′	41.2, CH_2	3.14, q (6.8)	41.3, CH_2	3.15, q (6.8)	41.3, CH_2	3.15, q (6.8)
2′	30.0, CH_2	1.46, m	30.0, CH_2	1.46, m	30.0, CH_2	1.47, m
3′	26.9, CH_2	1.27, m	26.9, CH_2	1.29, m	26.9, CH_2	1.28, m
4′	29.4, CH_2	1.25, m	29.4, CH_2	1.25, m	29.4, CH_2	1.26, m
5′	29.4, CH_2	1.25, m	29.5, CH_2	1.25, m	29.5, CH_2	1.26, m
6′	29.7, CH_2	1.25, m	29.7, CH_2	1.25, m	29.8, CH_2	1.26, m
7′	29.7, CH_2	1.25, m	29.7, CH_2	1.25, m	29.8, CH_2	1.26, m
8′	32.0, CH_2	1.25, m	29.7, CH_2	1.25, m	29.7, CH_2	1.26, m
9′	22.8, CH_2	1.29, m	32.0, CH_2	1.26, m	29.7, CH_2	1.26, m
10′	14.2, CH_3	0.88, t (6.8)	22.8, CH_2	1.30, m	32.1, CH_2	1.26, m
11′			14.2, CH_3	0.88, t (6.7)	22.8, CH_2	1.30, m
12′					14.3, CH_3	0.88, t (6.9)

Recorded at ^{1}H NMR 400 MHz and ^{13}C NMR 100 MHz in $CDCl_3$.

mg, 0.24 mmol, 96 %), **19** (77 mg, 0.24 mmol, 96 %), **20** (79 mg, 0.23 mmol, 94 %), **21** (84 mg, 0.24 mmol, 96 %), or **22** (87 mg, 0.24 mmol, 96 %).

4.6.1. 3,4-Dihydroxyphenethyl butylcarbamate (14)

Colorless oil; IR (ν_{max}) 3360, 3030, 2956, 1681, 1520, 1248, 1113 cm^{-1}; ^{1}H and ^{13}C NMR data see Table 8; HRESIMS *m/z* 276.1217 [M + Na]$^{+}$ (calcd for $C_{13}H_{19}NO_4Na^{+}$, 276.1212).

4.6.2. 3,4-Dihydroxyphenethyl pentylcarbamate (15)

Colorless oil; IR (ν_{max}) 3361, 3030, 2956, 1681, 1519, 1254, 1113 cm^{-1}; ^{1}H and ^{13}C NMR data see Table 8; HRESIMS *m/z* 290.1368 [M + Na]$^{+}$ (calcd for $C_{14}H_{21}NO_4Na^{+}$, 290.1368).

4.6.3. 3,4-Dihydroxyphenethyl hexylcarbamate (16)

Colorless oil; IR (ν_{max}) 3366, 3034, 2952, 1682, 1519, 1247, 1113 cm^{-1}; ^{1}H and ^{13}C NMR data see Table 8; HRESIMS *m/z* 304.1526 [M + Na]$^{+}$ (calcd for $C_{15}H_{23}NO_4Na^{+}$, 304.1525).

4.6.4. 3,4-Dihydroxyphenethyl heptylcarbamate (17)

Colorless amorphous solid; IR (ν_{max}) 3482, 3375, 3357, 2921, 1686, 1451, 1233, 1112 cm^{-1}; ^{1}H and ^{13}C NMR data see Table 9; HRESIMS *m/z* 318.1680 [M + Na]$^{+}$ (calcd for $C_{16}H_{25}NO_4Na^{+}$, 318.1681).

4.6.5. 3,4-Dihydroxyphenethyl octylcarbamate (18)

Colorless amorphous solid; IR (ν_{max}) 3461, 3375, 3349, 2913, 1693, 1449, 1240, 1112 cm^{-1}; ^{1}H and ^{13}C NMR data see Table 9; HRESIMS *m/z* 332.1842 [M + Na]$^{+}$ (calcd for $C_{17}H_{27}NO_4Na^{+}$, 332.1838).

4.6.6. 3,4-Dihydroxyphenethyl nonylcarbamate (19)

Colorless amorphous solid; IR (ν_{max}) 3439, 3297, 2956, 1690, 1527, 1257 cm^{-1}; ^{1}H and ^{13}C NMR data see Table 9; HRESIMS *m/z* 346.2005 [M + Na]$^{+}$ (calcd for $C_{18}H_{29}NO_4Na^{+}$, 346.1994).

4.6.7. 3,4-Dihydroxyphenethyl decylcarbamate (20)

Colorless amorphous solid; IR (ν_{max}) 3457, 3310, 2952, 1693, 1551, 1259, 1142 cm^{-1}; ^{1}H and ^{13}C NMR data see Table 10; HRESIMS *m/z* 360.2150 [M + Na]$^{+}$ (calcd for $C_{19}H_{31}NO_4Na^{+}$, 360.2151).

4.6.8. 3,4-Dihydroxyphenethyl undecylcarbamate (21)

Colorless amorphous solid; IR (ν_{max}) 3457, 3310, 3086, 2961, 1693, 1551, 1259, 1143 cm^{-1}; ^{1}H and ^{13}C NMR data see Table 10; HRESIMS *m/z* 374.2315 [M + Na]$^{+}$ (calcd for $C_{20}H_{33}NO_4Na^{+}$, 374.2307).

4.6.9. 3,4-Dihydroxyphenethyl dodecylcarbamate (22)

Colorless amorphous solid; IR (ν_{max}) 3457, 3310, 3077, 2918, 1694, 1552, 1258, 1143 cm^{-1}; ^{1}H and ^{13}C NMR data see Table 10; HRESIMS *m/z* 388.2455 [M + Na]$^{+}$ (calcd for $C_{21}H_{35}NO_4Na^{+}$, 388.2464).

4.7. Strains and media

Bloodstream forms of *T. b. brucei* 'single marker' S427 (S16) were grown at 37 °C under 5 % CO_2 in HMI-9 medium supplemented with 10 % heat-inactivated FBS (iFBS) [40].

L. donovani (MHOM/ET/67/HU3) with the luciferase gene integrated into the parasite genome (LUC) was grown at 28 °C in RPMI 1640-modified medium supplemented with 10 % iFBS and 50 mg/mL hygromycin B [41].

The MRC5-SV2 cell line (SV40-transformed human lung fibroblast cell line) was cultured in DMEM supplemented with 10 % iFBS, 100 U/mL penicillin, and 100 μg/mL streptomycin at 37 °C under 5 % CO_2.

THP-1, a human myelomonocytic cell line, was grown at 37 °C under 5 % CO_2 in RPMI-1640 medium supplemented with 10 % iFBS, 2 mM glutamate, 100 U/mL penicillin, and 100 mg/mL streptomycin.

4.8. Determination of cellular toxicity

THP-1 cells (3×10^4 cells/well) differentiated to macrophages with a treatment of 20 ng/mL PMA for 48 h, followed by 24 h of culture in fresh medium and MRC-5 cells (2×10^4 cells/well) were incubated in 96-well plates, in the presence of increasing concentrations of the different compounds, at 37 °C under 5 % of CO_2, for 72 h, and cell toxicity was determined using a resazurin-based assay [42]. Fluorescence was recorded using an Infinite® F200 microplate reader (Tecan Austria GmbH, Austria) with 550- and 590-nm filters.

The results are expressed as IC_{50}, which is defined as the concentration of the compound that reduces cell growth by 50 % compared with the untreated control cells. The assays were performed in two independent experiments performed in triplicate.

4.9. In vitro antitrypanosomal activity

The viability of *T. b. brucei* was measured by incubation of 2×10^4 parasites/well in 96-well microplates with increasing concentrations of drugs/compounds for 72 h at 37 °C under 5 % CO_2 in the culture medium. Cell proliferation was determined using a resazurin-based assay [43]. Fluorescence was recorded using an Infinite® F200 microplate

reader (Tecan Austria GmbH, Austria) with 550- and 590-nm filters. The results are expressed as IC_{50} values. The assays were performed in three independent experiments made in duplicate.

4.10. Susceptibility of the intracellular amastigote form of Leishmania

Macrophage-differentiated THP-1 cells were plated at a density of 3 $\times$ 10^4 macrophages/well in 96-well white polystyrene microplates and infected at a macrophage/parasite ratio of 1:10 with stationary L. *donovani* LUC promastigote form for 24 h at 35 °C under 5 % CO_2. Extracellular parasites were removed by washing with PBS (1.2 mM KH_2PO_4, 8.1 mM Na_2HPO_4, 130 mM NaCl, and 2.6 mM KCl, adjusted to pH 7.0). The infected cell cultures were then incubated in RPMI 1640 medium supplemented with 10 % iFBS at 37 °C under 5 % CO_2 for 72 h. To determine the susceptibility of L. *donovani* LUC amastigote, infected macrophages were lysed, and the luminescence intensity was measured as an indicator of intracellular parasite growth using a Luciferase Assay System Kit (Promega, Madison, Wisconsin, USA), as previously described [41]. Assays were performed in three independent experiments, and samples were collected in triplicate.

CRediT authorship contribution statement

Belinda Jimenez-Martin: Validation, Methodology, Investigation. **Diego A. Guerra-Arias:** Validation, Methodology, Investigation. **Antonio Martinez:** Supervision. **Raquel García-Hernández:** Methodology, Investigation, Data curation. **Marta Medina-O'Donnell:** Data curation. **José María Pérez-Victoria:** Writing – review & editing, Writing – original draft, Supervision, Funding acquisition, Conceptualization. **Francisco Rivas:** Writing – review & editing, Writing – original draft, Supervision, Funding acquisition, Conceptualization.

Declaration of competing interest

The authors declare that they have no known competing financial interests or personal relationships that could have appeared to influence the work reported in this paper.

Acknowledgments

This research was funded by grants from the Junta de Andalucia Consejeria de Economia Innovacion y Ciencia grant number B-FQM-650-UGR20 to FR, the National Plan for Scientific and Technical Research and Innovation 10.13039/501100011033 grant number PID2022-138474OB-I00 to JMPV, and FEDER funds from the EU to JMPV. We thank David Nesbitt for reviewing the English of the manuscript.

Appendix A. Supplementary data

Supplementary data (NMR data) to this article can be found online at https://doi.org/10.1016/j.bioorg.2025.108354.

Data availability

All data generated and analyzed during this study are included in this published article and its Supplementary material.

References

[1] CDCs Parasites, Parasitic Diseases. https://www.cdc.gov/parasites/index.html, 2024 accessed 20 Nov 2024.
[2] A. Tarannum, C.C. Rodríguez-Almonacid, J. Salazar-Bravo, Z.N. Karamysheva, Molecular mechanisms of persistence in protozoan parasites, Microorganisms 11 (2023) 2248, https://doi.org/10.3390/microorganisms11092248.
[3] J. Franco, L. Scarone, M.A. Comini, Drugs and drug resistance in african and american trypanosomiasis, Annu. Rep. Med. Chem. 51 (2018) 97–133, https://doi.org/10.1016/bs.armc.2018.08.003.
[4] L. Carvalho, M. Martinez-Garcia, I. Perez-Victoria, J.I. Manzano, V. Yardley, F. Gamarro, J.M. Perez-Victoria, The oral antimalarial drug tafenoquine shows activity against trypanosoma brucei, Antimicrob. Agents Chemother. 59 (2015) 6151–6160, https://doi.org/10.1128/aac.00879-15.
[5] N.J. Van Dijk, D.G. Hagos, D.M. Huggins, E. Carrillo, S. Ajala, C. Chicharro, D. Kiptanui, J.C. Solana, E. Abner, D. Wolday, H.D.F.H. Schallig, Simplified molecular diagnosis of visceral leishmaniasis: laboratory evaluation of miniature direct-on-blood PCR nucleic acid lateral flow immunoassay, PLoS Negl. Trop. Dis. 18 (2024) e0011637, https://doi.org/10.1371/journal.pntd.0011637.
[6] C. Maia, C. Conceição, A. Pereira, R. Rocha, M. Ortuño, C. Muñoz, Z. Jumakanova, P. Pérez-Cutillas, Y. Özbel, S. Töz, G. Baneth, B. Monge-Maillo, E. Gasimov, Y. Van der Stede, G. Torres, C.M. Gossner, E. Berriatua, The estimated distribution of autochthonous leishmaniasis by Leishmania infantum in Europe in 2005–2020, PLoS Negl. Trop. Dis. 17 (2023) e0011497, https://doi.org/10.1371/journal.pntd.0011497.
[7] M. Cabello-Donayre, S. Malagarie-Cazenave, J. Campos-Salinas, F.J. Gálvez, A. Rodríguez-Martínez, E. Pineda-Molina, L.M. Orrego, M. Martínez-García, M. P. Sánchez-Cañete, A.M. Estévez, J.M. Pérez-Victoria, Trypanosomatid parasites rescue heme from endocytosed hemoglobin through lysosomal HRG transporters, Mol. Microbiol. 101 (2016) 895–908, https://doi.org/10.1111/mmi.13430.
[8] A. Sain, S. Sahu, D. Naskar, Potential of olive oil and its phenolic compounds as therapeutic intervention against colorectal cancer: a comprehensive review, Brit. J. Nutr. 128 (2022) 1257–1273, https://doi.org/10.1017/S0007114521002919.
[9] F. Hadrich, M. Chamkha, S. Sayadi, Protective effect of olive leaves phenolic compounds against neurodegenerative disorders: promising alternative for Alzheimer and Parkinson diseases modulation, Food Chem. Toxicol. 159 (2022) 112752, https://doi.org/10.1016/j.fct.2021.112752.
[10] P. Rodríguez-López, J. Lozano-Sanchez, I. Borrás-Linares, T. Emanuelli, J. A. Menéndez, A. Segura-Carretero, Structure–biological activity relationships of extra-virgin olive oil phenolic compounds: health properties and bioavailability, Antioxidants 9 (2020) 685, https://doi.org/10.3390/antiox9080685.
[11] M. Stefani, S. Rigacci, Beneficial properties of natural phenols: highlight on protection against pathological conditions associated with amyloid aggregation, BioFactors 40 (2014) 482–493, https://doi.org/10.1002/biof.1171.
[12] S. Yu, G. Zhao, Development of polyphenols as HIV-1 integrase inhibitors: a summary and perspective, Curr. Med. Chem. 19 (2012) 5536–5561, https://doi.org/10.2174/092986712803833236.
[13] L. Micheli, L. Bertini, A. Bonato, N. Villanova, C. Caruso, M. Caruso, R. Bernini, F. Tirone, Role of hydroxytyrosol and oleuropein in the prevention of aging and related disorders: focus on neurodegeneration, skeletal muscle dysfunction and gut microbiota, Nutrients 15 (2023) 1767, https://doi.org/10.3390/nu15071767.
[14] N. Kumar, B. Gorai, S. Gupta, S. Goel, N. Goel, Extrapolation of hydroxytyrosol and its analogues as potential anti-inflammatory agents, J. Biomol. Struct. Dyn. 39 (2021) 5588–5599, https://doi.org/10.1080/07391102.2020.1792990.
[15] M. Bertelli, A.K. Kiani, S. Paolacci, E. Manara, D. Kurti, K. Dhuli, V. Bushati, J. Miertus, D. Pangallo, M. Baglivo, T. Beccari, S. Michelini, Hydroxytyrosol: a natural compound with promising pharmacological activities, J. Biotechnol. 309 (2020) 29–33, https://doi.org/10.1016/j.jbiotec.2019.12.016.
[16] R. Bernini, N. Merendino, A. Romani, F. Velotti, Naturally occurring hydroxytyrosol: synthesis and anticancer potential, Curr. Med. Chem. 20 (2013) 655–670, https://doi.org/10.2174/092986713804999367.
[17] M. Nardi, S. Brocchini, S. Somavarapu, A. Procopio, Hydroxytyrosol oleate: a promising neuroprotective nanocarrier delivery system of oleuropein and derivatives, Int. J. Pharm. 631 (2023) 122498, https://doi.org/10.1016/j.ijpharm.2022.122498.
[18] D.Y. Zhou, Y.X. Sun, F. Shahidi, Preparation and antioxidant activity of tyrosol and hydroxytyrosol esters, J. Funct. Foods 37 (2017) 66–73, https://doi.org/10.1016/j.jff.2017.06.042.
[19] R. Bernini, I. Carastro, G. Palmini, A. Tanini, R. Zonefrati, P. Pinelli, M.L. Brandi, A. Romani, Lipophilization of hydroxytyrosol-enriched fractions from Olea europaea L. byproducts and evaluation of the in vitro effects on a model of colorectal cancer cells, J. Agric. Food Chem. 65 (2017) 6506–6512, https://doi.org/10.1021/acs.jafc.6b05457.
[20] M. Candiracci, A. Madrona, J.L. Espartero, G. Zappia, E. Piatti, Lipophilic hydroxytyrosol esters significantly improve the oxidative state of human red blood cells, J. Funct. Foods 23 (2016) 339–347, https://doi.org/10.1016/j.jff.2016.02.049.
[21] R. Bernini, F. Crisante, N. Merendino, R. Molinari, M.C. Soldatelli, F. Velotti, Synthesis of a novel ester of hydroxytyrosol and α-lipoic acid exhibiting an antiproliferative effect on human colon cancer HT-29 cells, Eur. J. Med. Chem. 46 (2011) 439–446, https://doi.org/10.1016/j.ejmech.2010.10.028.
[22] S. Vicinanza, F. Annunziata, D. Pecora, A. Pinto, L. Tamborini, Lipase-mediated flow synthesis of nature-inspired phenolic carbonates, RSC Adv. 13 (2023) 22901–22904, https://doi.org/10.1039/d3ra04735k.
[23] I. Fernandez-Pastor, A. Fernandez-Hernandez, F. Rivas, A. Martinez, A. Garcia-Granados, A. Parra, Synthesis and antioxidant activity of hydroxytyrosol alkyl-carbonate derivatives, J. Nat. Prod. 79 (2016) 1737–1745, https://doi.org/10.1021/acs.jnatprod.6b00124.
[24] R. Cert, A. Madrona, J.L. Espartero, M.C. Pérez-Camino, Antioxidant activity of alkyl hydroxytyrosyl ethers in unsaturated lipids, Food Funct. 6 (2015) 1999–2007, https://doi.org/10.1039/C5FO00300H.
[25] J.M. Calderon-Montano, A. Madrona, E. Burgos-Moron, M.L. Orta, S. Mateos, J. L. Espartero, M. Lopez-Lazaro, Selective cytotoxic activity of new lipophilic

hydroxytyrosol alkyl ether derivatives, J. Agric. Food Chem. 61 (2013) 5046–5053, https://doi.org/10.1021/jf400796p.
[26] G. Pereira-Caro, L. Bravo, A. Madrona, J.L. Espartero, R. Mateos, Uptake and metabolism of new synthetic lipophilic derivatives, hydroxytyrosyl ethers, by human hepatoma HepG2 cells, J. Agric. Food Chem. 58 (2010) 798–806, https://doi.org/10.1021/jf902690z.
[27] R. Bernini, M.S.G. Montani, N. Merendino, A. Romani, F. Velotti, Hydroxytyrosol-derived compounds: a basis for the creation of new pharmacological agents for cancer prevention and therapy, J. Med. Chem. 58 (2015) 9089–9107, https://doi.org/10.1021/acs.jmedchem.5b00669.
[28] I. Fernandez-Pastor, M. Martínez-García, M. Medina-O'Donnell, F. Rivas, A. Martinez, J.M. Pérez-Victoria, A. Parra, Semisynthesis of ω-hydroxyalkylcarbonate derivatives of hydroxytyrosol as antitrypanosome agents, J. Nat. Prod. 81 (2018) 2075–2082, https://doi.org/10.1021/acs.jnatprod.8b00431.
[29] E. Belmonte-Reche, M. Martinez-Garcia, P. Peñalver, V. Gomez-Perez, R. Lucas, F. Gamarro, J.M. Perez-Victoria, J.C. Morales, Tyrosol and hydroxytyrosol derivatives as antitrypanosomal and antileishmanial agents, Eur. J. Med. Chem. 119 (2016) 132–140, https://doi.org/10.1016/j.ejmech.2016.04.047.
[30] A.K. Ghosh, M. Brindisi, Organic carbamates in drug design and medicinal chemistry, J. Med. Chem. 58 (2015) 2895–2940, https://doi.org/10.1021/jm501371s.
[31] S. Vicinanza, L. Mombelli, F. Annunziata, S. Donzella, M.L. Contente, C. Borsari, P. Conti, G. Meroni, F. Molinari, P.A. Martino, A. Pinto, L. Tamborini, Chemo-enzymatic flow synthesis of nature-inspired phenolic carbonates and carbamates as antiradical and antimicrobial agents, Sustain. Chem. Pharm. 39 (2024) 101542, https://doi.org/10.1016/j.scp.2024.101542.
[32] M. De Rycker, I. Hallyburton, J. Thomas, L. Campbell, S. Wyllie, D. Joshi, S. Cameron, I.H. Gilbert, P.G. Wyatt, J.A. Frearson, A.H. Fairlamb, D.W. Gray, Comparison of a high-throughput high-content intracellular Leishmania donovani assay with an axenic amastigote assay, Antimicrob. Agents Chemother. 57 (2013) 2913–2922, https://doi.org/10.1128/aac.02398-12.
[33] T.T. Pham, M. Walden, C. Butler, R. Diaz-Gonzalez, G. Perez-Moreno, G. Ceballos-Perez, V. Gomez-Perez, R. Garcia-Hernandez, H. Zecca, E. Krakoff, B. Kopec, O. Ichire, C. Mackenzie, M. Pitot, L.M. Ruiz, F. Gamarro, D. Gonzalez-Pacanowska, M. Navarro, A.B. Dounay, Novel 1,2-dihydroquinazolin-2-ones: design, synthesis, and biological evaluation against Trypanosoma brucei, Bioorg. Med. Chem. Lett. 27 (2017) 3629–3635, https://doi.org/10.1016/j.bmcl.2017.07.032.
[34] N. Wiedemar, D.A. Hauser, P. Mäser, 100 years of Suramin, Antimicrob. Agents Chemother. 64 (2020), https://doi.org/10.1128/AAC.01168-19 e01168–19.
[35] J.Q. Reimão, D.P. Pita Pedro, A.C. Coelho, The preclinical discovery and development of oral miltefosine for the treatment of visceral leishmaniasis: a case history, expert Opin, Drug Des. Discov. 15 (2020) 647–658, https://doi.org/10.1080/17460441.2020.1743674.
[36] N.K. Verma, C.S. Dey, Possible mechanism of miltefosine-mediated death of Leishmania donovani, Antimicrob. Agents Chemother. 48 (2004) 3010–3015, https://doi.org/10.1128/aac.48.8.3010-3015.2004.
[37] I.M. de Melo, T.P. Camargo, V.A. da Silva, E.G. dos Santos, I.S. Caldas, C.L. M. Pontes, P.H. Stoco, M.M. Vaidergorn, M.C. Nonato, T.B. de Souza, Discovery of a new eugenol-benznidazole hybrid active against different evolutive stages of Trypanosoma cruzi, Bioorg. Chem. 154 (2025) 107993, https://doi.org/10.1016/j.bioorg.2024.107993.
[38] K. Katsuno, J.N. Burrows, K. Duncan, R.H. van Huijsduijnen, T. Kaneko, K. Kita, C. E. Mowbray, D. Schmatz, P. Warner, B.T. Slingsby, Hit and lead criteria in drug discovery for infectious diseases of the developing world, Nat. Rev. Drug Discov. 14 (2015) 751–758, https://doi.org/10.1038/nrd4683.
[39] A. Garcia-Granados, A. Parra, Method for the industrial use of tyrosol and hydroxytyrosol contained in the solid by-products of industrial olive crushing, PCT Int. Appl. WO (2007), 2007093659.
[40] E. Wirtz, S. Leal, C. Ochatt, G.A.M. Cross, A tightly regulated inducible expression system for conditional gene knock-outs and dominant-negative genetics in Trypanosoma brucei, Mol. Biochem. Parasitol. 99 (1999) 89–101, https://doi.org/10.1016/S0166-6851(99)00002-X.
[41] R. García-Hernández, V. Gómez-Pérez, S. Castanys, F. Gamarro, Fitness of Leishmania donovani parasites resistant to drug combinations, PLoS Negl. Trop. Dis. 9 (2015) e0003704, https://doi.org/10.1371/journal.pntd.0003704.
[42] E.M. Sanchez-Fernandez, V. Gomez-Perez, R. Garcia-Hernandez, J.M. Garcia Fernandez, G.B. Plata, J.M. Padrón, C. Ortiz Mellet, S. Castanys, F. Gamarro, Antileishmanial activity of sp^2-iminosugar derivatives, RSC Adv. 5 (2015) 21812–21822, https://doi.org/10.1039/C5RA02627J.
[43] B. Raz, M. Iten, Y. Grether-Buhler, R. Kaminsky, R. Brun, The Alamar blue assay to determine drug sensitivity of African trypanosomes (T.B. Rhodesiense and T.B. Gambiense) in vitro, Acta Trop. 68 (1997) 139–147, https://doi.org/10.1016/S0001-706X(97)00079-X.